

Video Article

Aerosol-assisted Chemical Vapor Deposition of Metal Oxide Structures: Zinc Oxide Rods

Stella Vallejos^{1,2}, Naděžda Pizúrová³, Jan Čechal⁴, Isabel Gràcia¹, Carles Cané¹¹Instituto de Microelectrónica de Barcelona (IMB-CNM, CSIC)²SIX Research Centre, Brno University of Technology³Institute of Physics of Material, Academy of Science of Czech Republic⁴Institute of Physical Engineering and Central European Institute of Technology, Brno University of TechnologyCorrespondence to: Stella Vallejos at vargas@feec.vutbr.czURL: <https://www.jove.com/video/56127>DOI: [doi:10.3791/56127](https://doi.org/10.3791/56127)

Keywords: Chemistry, Issue 127, Zinc oxide, columnar structures, rods, AACVD, non-catalyzed growth, vapor-solid mechanism

Date Published: 9/14/2017

Citation: Vallejos, S., Pizúrová, N., Čechal, J., Gràcia, I., Cané, C. Aerosol-assisted Chemical Vapor Deposition of Metal Oxide Structures: Zinc Oxide Rods. *J. Vis. Exp.* (127), e56127, doi:10.3791/56127 (2017).

Abstract

Whilst columnar zinc oxide (ZnO) structures in the form of rods or wires have been synthesized previously by different liquid- or vapor-phase routes, their high cost production and/or incompatibility with microfabrication technologies, due to the use of pre-deposited catalyst-seeds and/or high processing temperatures exceeding 900 °C, represent a drawback for a widespread use of these methods. Here, however, we report the synthesis of ZnO rods *via* a non-catalyzed vapor-solid mechanism enabled by using an aerosol-assisted chemical vapor deposition (CVD) method at 400 °C with zinc chloride (ZnCl₂) as the precursor and ethanol as the carrier solvent. This method provides both single-step formation of ZnO rods and the possibility of their direct integration with various substrate types, including silicon, silicon-based micromachined platforms, quartz, or high heat resistant polymers. This potentially facilitates the use of this method at a large-scale, due to its compatibility with state-of-the-art microfabrication processes for device manufacture. This report also describes the properties of these structures (*e.g.*, morphology, crystalline phase, optical band gap, chemical composition, electrical resistance) and validates its gas sensing functionality towards carbon monoxide.

Video Link

The video component of this article can be found at <https://www.jove.com/video/56127/>

Introduction

ZnO is a II - VI semiconductor with a wide direct band gap (3.37 eV), large exciton binding energy (60 meV), spontaneous polarization and piezoelectric constants that make it an attractive material for electronics, optoelectronics, energy generators, photocatalysis and chemical sensing. Most of the interesting functionalities of ZnO are related to its wurtzite crystal structure and its non-polar (*e.g.*, {100}, {110}) and polar (*e.g.*, {001}, {111}) surfaces associated to specific structured morphological forms (*e.g.*, rods, pyramids, plates). The control of these morphological forms requires synthetic methods capable of producing well-defined crystals, with uniform size, shape, and surface structure^{1,2,3,4}. In this context, new additive (bottom-up synthesis) manufacturing strategies, particularly based on vapor-phase routes are industrially attractive and potentially advantageous as they provide the ability to generate structured films in a continuous rather than batch mode with high purity and high throughputs. These routes have demonstrated the formation of ZnO structured films previously, but usually employing catalyst-seeds such as gold and/or high processing temperatures of 900 - 1,300 °C² {Wang, 2008 #491} (this might be inconvenient for certain fabrication processes due to the need of extra processing steps and/or temperature incompatibilities for in-chip integration).

Recently, we have used a vapor-phase method based on aerosol-assisted CVD of inorganic or metal-organic precursors to achieve the selective deposition of metal oxide structures (*e.g.*, tungsten oxide⁵ or tin oxide⁶), without the need of catalyst-seeds and at lower temperatures than those reported for traditional CVD. This method works at atmospheric pressure and can use less-volatile precursors compared to traditional CVD; solubility is the key precursor requirement, as the precursor solution is delivered to the reaction zone in an aerosol form⁷. In aerosol-assisted CVD, the nucleation and growth kinetics of structured materials and thin films are influenced by the synthesis temperature and concentration of reactive species, which in turn influence the morphological form of the film⁸. Recently, we have studied the morphology dependence of ZnO to various aerosol-assisted CVD conditions (including precursors, temperatures, carrier solvents, and precursor concentrations) and found routes for the formation of structured ZnO with rods-, flakes-, or upside-down-cone-like morphologies, among others⁹.

Herein, we present the protocol for the aerosol-assisted CVD of columnar ZnO structures in the form of rods composed in the majority by {100} surfaces. This protocol is compatible with various substrates including silicon, silicon-based micromachined platforms, quartz, or high heat resistant polyimide foils. In this report, we focus on the coating of bare silicon wafers and silicon-based micromachined platforms employed for the fabrication of gas sensors. The aerosol-assisted CVD of ZnO consists of three processing steps that include: the preparation of substrates and set-up of deposition temperature, the preparation of the solution for aerosol generation, and the CVD process. These steps are described in detail below and a schematic view showing the main elements of the system is displayed in **Figure 1**.

Protocol

Notes: For safety reasons, the reaction cell and the aerosol generator are placed inside a fume hood. Employ tweezers to handle the samples, wear gloves, a lab-coat, and goggles, and follow common laboratory safety practices.

1 . Preparation of Substrates and Set-up of Deposition Temperature

1. Cut 10 mm x 10 mm silicon substrates using a diamond tip scribe (the substrate dimensions have been adapted to the size of our reaction cell). For this experiment, use a home-made stainless steel cylindrical reaction cell with an internal volume of $\sim 7,000 \text{ mm}^3$ (diameter: 30 mm, height: 10 mm) adapted to the dimensions of the silicon-based micromachined platforms employed for the fabrication of gas sensors.
2. Clean the substrates in isopropanol, rinse with deionized water, and blow-dry the substrates with nitrogen to ensure good adherence of the films and uniform covering of the substrate.
3. Place the substrate into the reaction cell. When using silicon-based micromachined platforms, instead of bare silicon substrates for the fabrication of gas sensors, place the micromachined platforms into the reaction cell and then align with a shadow mask to confine the growth of material to the area of interest.
4. Close the reaction cell. Make sure that the lid of the reaction cell is properly sealed to avoid the leakage of reactive species.
5. Switch-on the temperature control system, consisting of resistive heaters integrated with the reaction cell, a thermocouple to sense the temperature of the substrate and a proportional-integral-derivative (PID) controller.
6. Set the temperature to 400 °C and let it to stabilize (this process takes approximately 30 min, but it may change depending on the reaction cell dimensions and the characteristics of the temperature control system).

2 . Preparation of Solution for Aerosol Generation

1. Add 50 mg of ZnCl_2 to a 100 mL glass vial equipped with a vacuum trap (29/32 joint, 200 mm length, 5 mm hose barbs).
2. Dissolve the ZnCl_2 in 5 mL of ethanol and then cap the vial with the vacuum trap. Ensure the down-pipe end sits 60 mm above the bottom of the vial and without submerging in the solution. If needed, employ glass joint clips to secure the vial and the vacuum trap together during the CVD process.
3. Clamp the vial to a universal support. Adjust the height to meet the bottom of the vial and the optimal focal point of the ultrasonic atomizer that operates at 1.6 MHz and delivers an average size of the aerosol droplets of $\#3 \mu\text{m}$.
4. Connect the inlet and the exhaust of the vacuum trap to the nitrogen pipe and the reaction cell, respectively, as shown in the simplified scheme of the aerosol-assisted CVD system in **Figure 1**.
5. Use a fresh solution of reactants for each deposition.

3 . CVD Process

1. Before starting the CVD process, verify that the temperature in the reaction cell has reached the steady state.
2. Adjust the nitrogen flow to $200 \text{ cm}^3/\text{min}$ and allow it to flow through the system (the flow rate has been tuned according to the dimensions of the reaction cell used in our experiments). The use of a mass-flow controller is recommended to ensure a constant flow during the deposition.
3. Switch-on the aerosol generator and keep the aerosol constant during the process until the solution containing the zinc precursor is completely delivered to the reaction cell (this process takes approximately 120 min considering a solution volume of 5 mL and a flow rate of $200 \text{ cm}^3/\text{min}$).
4. As soon as the solution has been fully delivered to the reaction cell, switch-off the aerosol generator and the temperature system to cool down the reaction cell. Meanwhile keep the nitrogen flowing throughout the system.
5. When the temperature has dropped to room temperature, close the nitrogen flow, open the reaction cell, and remove the samples. The substrate will show a greyish matte color on the surface, different from the shiny bare silicon wafer (the silicon-based micromachined platforms display a similar appearance after the CVD step). This matte color is associated with the presence of columnar ZnO structures in the form of rods like those observed by scanning electron microscopy (**Figure 2**).

Representative Results

The aerosol-assisted CVD of ZnCl_2 dissolved in ethanol leads to the formation of greyish uniform and adherent films on bare silicon wafers (relatively easily abraded mechanically). Characterization of the films using scanning electron microscopy (SEM) above 8,000X magnification displays quasi-aligned hexagonal shaped ZnO rods with lengths of $\#1,600$ and diameters of $\#380 \text{ nm}$ (**Figure 2**). Large errors in the set-point temperature or the presence of temperature gradients along the substrate during the CVD may cause the deposition of other ZnO morphologies (**Figure 3**) or films with non-uniform structures. In addition, uneven or non-adherent coatings may be related in part to poor temperature control, incorrect adjustment of the flow, and/or the use of a different carrier solvent than that specified in this protocol.

X-ray diffraction (XRD) analysis of the rods shows diffraction patterns associated with a hexagonal ZnO phase ($P6_3mc$ space group, $a = 3.2490 \text{ \AA}$, $b = 3.2490 \text{ \AA}$, and $c = 5.2050 \text{ \AA}$; ICDD Card No. 5-0664). These patterns display a high intensity diffraction peak at $34.34^\circ 2\theta$, corresponding to the (002) plane of the hexagonal ZnO phase, along with other seven low intensity diffraction peaks at 31.75 , 36.25 , 47.54 , 56.55 , 62.87 , 67.92 , and $72.61^\circ 2\theta$, corresponding to the (100) (101) (102) (110) (103) (201) and (004) planes of the hexagonal ZnO phase, respectively. Characterization of the rods by high-resolution transmission electron microscopy (TEM) shows marked planar spacing (0.26 nm) consistent with the internal lattice of the (002) plane ($d = 0.26025 \text{ nm}$) of the hexagonal ZnO phase identified by XRD. Energy-dispersive X-ray (EDX) spectroscopy shows the presence of Zn with relatively low chlorine contamination (found for Cl:Zn 0.05 at.%).

The estimation of the optical bandgap of the rods by means of diffuse reflectance measurements of films indicates an optical bandgap of 3.2 eV, consistent with the literature values for ZnO¹⁰. The analysis of the films using X-ray photoelectron spectroscopy (XPS) is characterized by Zn 2p_{1/2} and Zn 2p_{3/2} core level peaks spectra at 1,045 and 1,022 eV, respectively, consistent with those observed previously for ZnO^{11,12}.

The use of this protocol on silicon-based micromachined platforms intended for gas sensing lead to the direct integration of columnar ZnO rods confined on the sensing-active area (400 x 400 μm²), which is defined by a shadow mask. The electrical resistance of the films is in the order of kΩ (# 100 kΩ) measured at room temperature by using the interdigitated electrodes integrated into the silicon-based micromachined platforms. **Figure 4** displays the picture of an array of four micromachined gas sensors based on aerosol-assisted CVD rods. The characteristics and fabrication process for the micromachined platforms have been described previously¹³. These microsystems are sensitive to relative low concentrations of carbon monoxide, with the maximum responses recorded (using a continuous gas flow test chamber¹³) when the sensors were operated at 360 °C using the resistive microheaters integrated in the system (**Figure 5**).

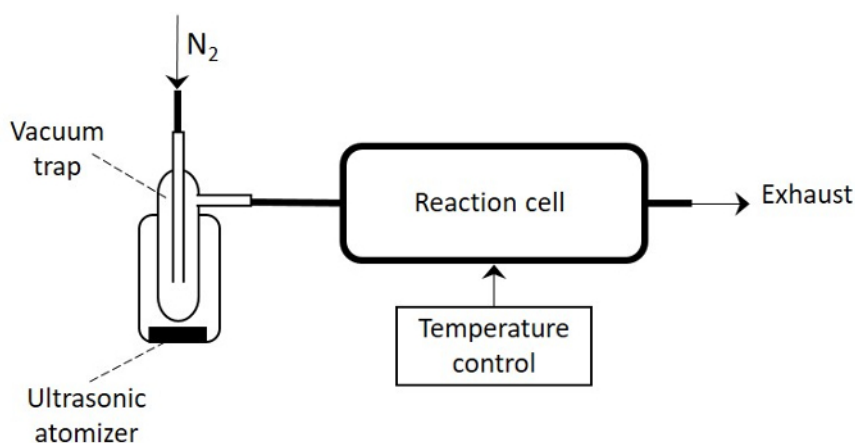


Figure 1: Schematic View of the Aerosol-assisted CVD System.

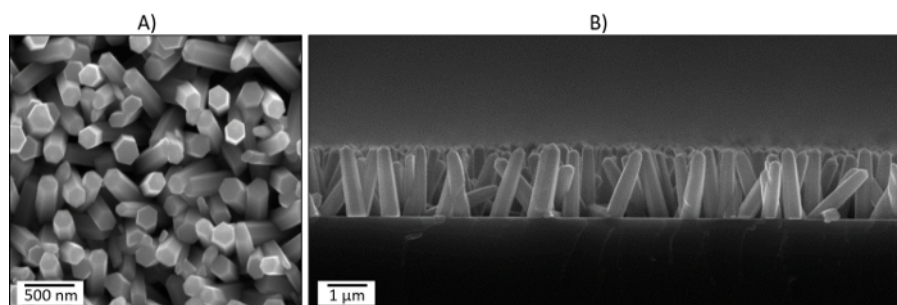


Figure 2: Top (A) and Cross-sectional (B) SEM Images of the ZnO Rods Deposited via Aerosol-Assisted CVD. [Please click here to view a larger version of this figure.](#)

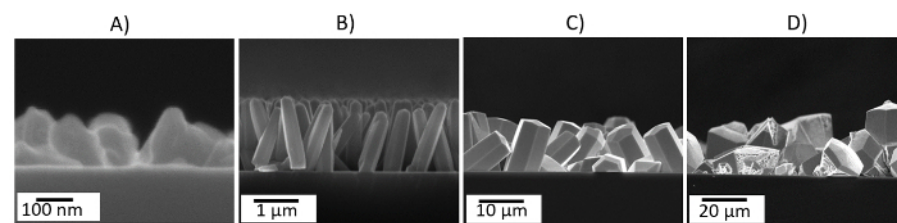


Figure 3: Cross-sectional SEM Images of ZnO Deposited via Aerosol-assisted CVD at 300 (A), 400 (B), 500 (C), and 600 °C (D). [Please click here to view a larger version of this figure.](#)

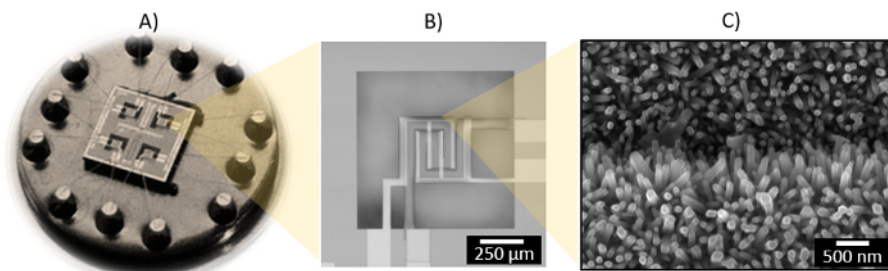


Figure 4: Silicon-based Micromachined Platform with 4 Microsensors Mounted on a TO8-package (A), and Detailed View of a Microsensor (B) and the ZnO Rods Deposited on the Edge of an Electrode (C). [Please click here to view a larger version of this figure.](#)

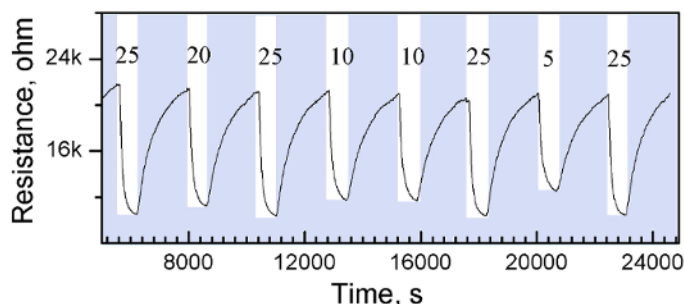


Figure 5: Electrical Resistance Changes of the ZnO Rods Towards Various Concentrations (25, 20, 10 and 5 ppm) of Carbon Monoxide. [Please click here to view a larger version of this figure.](#)

Discussion

The aerosol-assisted CVD procedure detailed here leads to the formation of ZnO rods on silicon tiles of 10 mm x 10 mm. This procedure can be scaled-up to coat larger surfaces; however, notice that an increase in the reaction cell volume will require a readjustment of parameters, such as the carrier flow rate and the volume of solution. For larger reaction cells, it is also recommended to control the temperature gradients in the substrate, due to subtle gradients of less than 10 °C possibly having a strong influence on the resulting morphology of the film, as demonstrated previously for the aerosol-assisted CVD of tungsten oxide⁸. To reproduce the results reported here, we recommend the use of an ultrasonic atomizer with similar operating frequency than that described in the protocol, as the average droplet size of the aerosol and in turn the resulting morphology of the film are influenced by this parameter⁷.

The selective deposition of other ZnO morphologies, rather than rods, can also be achieved by changing the precursor, deposition temperatures, or carrier solvents. For instance, the use of precursors such as diethyl zinc¹⁴ or zinc acetate¹⁵ has proved to lead to the formation of other morphological forms rather than hexagonal rods. We have also noticed that the use of different deposition temperatures during aerosol-assisted CVD produces changes in the morphology of the films, allowing for the formation of polycrystalline films at temperatures below 400 °C, thicker hexagonal structures at temperatures exceeding 400 °C, or degraded and less dense structures on the substrate when reaching 600 °C. Similarly, the use of different solvents influences the morphology of the films, and for instance, we have proved recently that the use of methanol at the deposition temperature of 400 °C encourages the formation of structures with flake-like morphology, whereas the use of acetone at the same temperature encourages the formation of upside-down cone-like structures⁹.

The role of the temperature and carrier solvents was also noticed previously on the aerosol-assisted CVD of other metal oxides structures (e.g., tungsten oxide⁵ and tin oxide⁶), and it was generally attributed to: chemical effects caused by reactive intermediates, which become active species for deposition or react homogeneously to form solid particles at the processing temperatures (this is more likely for solvents such as methanol and acetone, which can decompose at low temperatures e.g., <500 °C); and modulation of the rates of deposition (flux) and droplet evaporation (this is more likely dominant for solvents as ethanol, which do not form reactive radical species at the temperatures used in our experiments).

The protocol reported here is compatible with state-of-the-art microfabrication processes for silicon-based electronic devices and has the potential to be incorporated in processes involving high heat resistant flexible materials due to the relatively low temperatures for the aerosol-assisted CVD of structures. However, it is important to mention that the use of shadow masks for the selective growth of structures, such as in seeded methods based on the vapor-liquid-solid mechanism¹⁶, may have constraints in certain fabrication processes. On the other hand, the possibility to grow the structures via the non-catalyzed method presented here may have the advantage of less lithographic and metallization steps for in-chip integration of structures. Additionally, the relative low temperatures for the synthesis of ZnO rods may also allow for the use of this method with localized heating, a technique employed to confine the required thermal environment for both decomposition of the vapor-phase reactants and the growth kinetics of structures to a microscale area, reducing significantly the power consumption of high temperature (hot-wall) reactors¹⁷. The use of localized heating, for instance, has been shown feasible previously for the non-catalyzed aerosol-assisted CVD of tungsten oxide rods¹⁸. The growth of columnar ZnO structures with controlled morphology, that allow for their easy integration into different substrate and microfabrication processes, is of common interest in areas such as chemical sensing, photocatalysis, photonics and energy harvesting, amongst others.

Disclosures

The authors have nothing to disclose

Acknowledgements

This work has been supported in part by the Spanish Ministry of Science and Innovation via Grant TEC2015-74329-JIN-(AEI/FEDER,EU), TEC2016-79898-C6-1-R (AEI/FEDER, EU), and TEC-2013-48147-C6-6R (AEI/FEDER, EU). SV acknowledges the support of the SoMoPro II Programme, co-financed by the European Union and the South Moravian Region, via Grant 4SGA8678. JČ acknowledges the funding provided by MEYS, Project No. LQ1601 (CEITEC 2020). Part of this research has made use of the infrastructures of the SIX Research Centre, the core facilities of CEITEC under CEITEC-open access project via Grant LM2011020 funded by the Ministry of Education, Youth and Sports of the Czech Republic, and the Spanish ICTS Network MICRONANOFABS partially supported by MINECO.

References

1. Kozuka, Y., Tsukazaki, A., Kawasaki, M. Challenges and opportunities of ZnO-related single crystalline heterostructures. *Appl Phys Rev.* **1**(1), 011303 (2014).
2. Wang, Z. L. Splendid One-Dimensional Nanostructures of Zinc Oxide: A New Nanomaterial Family for Nanotechnology. *ACS Nano.* **2**(10), 1987-1992 (2008).
3. Pal, J., Pal, T. Faceted metal and metal oxide nanoparticles: design, fabrication and catalysis. *Nanoscale.* **7**(34), 14159-14190 (2015).
4. Sun, Y., *et al.* The Applications of Morphology Controlled ZnO in Catalysis. *Catalysts.* **6**(12), 188 (2016).
5. Vallejos, S., Umek, P., Blackman, C. AACVD Control parameters for selective deposition of tungsten oxide nanostructures. *J Nanosci Nanotechnol.* **11** 8214-8220 (2011).
6. Vallejos, S., *et al.* Aerosol assisted chemical vapour deposition of gas sensitive SnO₂ and Au-functionalised SnO₂ nanorods via a non-catalysed vapour solid (VS) mechanism. *Sci Rep.* **6** 28464, 28461-28412 (2016).
7. Hou, X., Choy, K. L. Processing and Applications of Aerosol-Assisted Chemical Vapor Deposition. *Chem Vap Deposition.* **12**(10), 583-596 (2006).
8. Ling, M., Blackman, C. Growth mechanism of planar or nanorod structured tungsten oxide thin films deposited via aerosol assisted chemical vapour deposition (AACVD). *Phys Status Solidi C.* **12**(7), 869-877 (2015).
9. Vallejos, S., *et al.* ZnO Rods with Exposed {100} Facets Grown via a Self-Catalyzed Vapor-Solid Mechanism and Their Photocatalytic and Gas Sensing Properties. *ACS Appl Mater Inter.* **8**(48), 33335-33342 (2016).
10. Srikant, V., Clarke, D. R. On the optical band gap of zinc oxide. *J Appl Phys.* **83**(10), 5447-5451 (1998).
11. Gogurla, N., Sinha, A. K., Santra, S., Manna, S., Ray, S. K. Multifunctional Au-ZnO Plasmonic Nanostructures for Enhanced UV Photodetector and Room Temperature NO Sensing Devices. *Sci Rep.* **4** 6483, 6481-6489 (2014).
12. Sutka, A., *et al.* A straightforward and "green" solvothermal synthesis of Al doped zinc oxide plasmonic nanocrystals and piezoresistive elastomer nanocomposite. *RSC Advances.* **5**(78), 63846-63852 (2015).
13. Vallejos, S., *et al.* Chemoresistive micromachined gas sensors based on functionalized metal oxide nanowires: Performance and reliability. *Sens Actuator B.* **235** 525-534 (2016).
14. Bhachu, D. S., Sankar, G., Parkin, I. P. Aerosol Assisted Chemical Vapor Deposition of Transparent Conductive Zinc Oxide Films. *Chem Mater.* **24**(24), 4704-4710 (2012).
15. Chen, S., Wilson, R. M., Binions, R. Synthesis of highly surface-textured ZnO thin films by aerosol assisted chemical vapour deposition. *J Mater Chem. A.* **3**(11), 5794-5797 (2015).
16. Murillo, G., Rodríguez-Ruiz, I., Esteve, J. Selective Area Growth of High-Quality ZnO Nanosheets Assisted by Patternable AlN Seed Layer for Wafer-Level Integration. *Cryst Growth Des.* **16**(9), 5059-5066 (2016).
17. Sosnowchik, B. D., Lin, L., Englander, O. Localized heating induced chemical vapor deposition for one-dimensional nanostructure synthesis. *J Appl Phys.* **107**(5) (2010).
18. Annanouch, F. E., *et al.* Localized aerosol-assisted CVD of nanomaterials for the fabrication of monolithic gas sensor microarrays. *Sens Actuators, B.* **216** 374-383 (2015).